| | |
|---|---|
| **Preprint Title** | Revisiting the Algar-Flynn-Oyamada (AFO) Reaction Mechanism: Computational and other Studies |
| **Authors** | Carla Teixeira, Sergio Sousa and Anthony J. Burke |
| **Publication Date** | 24 Apr. 2024 |
| **Article Type** | Full Research Paper |
| **Supporting Information File 1** | Supporting Information Burke et al.docx; 43.3 KB |
| **ORCID® iDs** | Carla Teixeira - https://orcid.org/0000-0002-8422-9392; Sergio Sousa - https://orcid.org/0000-0002-6560-5284; Anthony J. Burke - https://orcid.org/0000-0001-8248-1116 |

# Revisiting the Algar-Flynn-Oyamada (AFO) Reaction Mechanism: Computational and other Studies

Carla S. S. Teixeira[a], Sergio F. Sousa[a] Anthony J. Burke[b,c,d,e, f*]

[a] LAQV/REQUIMTE, BioSIM – Department of Biomedicine, Faculty of Medicine, Universidade do Porto, Alameda Prof. Hernâni Monteiro, 4200-319 Porto, Portugal. (Sérgio F. Sousa: 0000-0002-6560-5284; Carla S. S. Teixeira: 0000-0002-8422-9392)

[b]Faculty of Pharmacy, University of Coimbra, Pólo das Ciências da Saúde, Azinhaga de Santa Coimbra, 3000-548 Coimbra, Portugal.

[c]Coimbra chemistry centre, Institute of Molecular Sciences, Rua Larga, 3004-535 Coimbra, Portugal.

[d]LAQV-REQUIMTE, Institute for Research and Advanced Studies, Universidade de Évora, Rua Romão Romalho 59, 7000 Évora, Portugal.

[e]Center for Neurosciences and Cellular Biology (CNC), Polo I, Universidade de Coimbra Rua Larga Faculdade de Medicina, Polo I, 1°andar 3004–504, Coimbra Portugal.
ajburke@ff.uc.pt
[f] Department of Chemistry, University College, Belfield, Dublin 4, Ireland.

*Abstract*
The flavonoid family is a diverse family of natural phenolic compounds, with multiple biological properties. Both flavonols and aurones and their derivatives are key flavonoid compounds. These molecules traditionally have been obtained through the classical Algar, Flynn and Oyamada (AFO) reaction by treatment of 2'-hydroxychalcones with alkaline hydrogen peroxide. The mechanism is controversial, with indications of the formation of an epoxide intermediate when there is a substituent in the 6'-position (giving aurones and other benzofuran-2-one derivatives), and in the case of the 6'-substituted substratesan oxidative cyclization (directly or step-wise) involving no epoxide intermediates to give flavanols (Dean and Podimuang mechanism). In this paper, the mechanism of this reaction was studied computationally (DFT calculations) and the results indicated that for the unsubstituted systems the Dean and Podimuang mechanism is favoured both kinetically and thermodynamically, but in the case of the substituted systems, although the former mechanism is again favoured kinetically, both mechanisms show similar energies at the thermodynamic level, indicating that both the Dean and Podimuang mechanism and the epoxide forming pathway may operate in parallel. Interestingly, the calculations indicated an unexpected electrophilic hydroperoxide epoxidation route instead of a nucleophilic epoxidation route. Modified AFO conditions were studied whereby $H_2O_2$ was replaced by *m*CPBA, these experiments afforded mainly flavanone and some AFO products in low yields.

**Introduction**

The synthesis of flavonoid compounds has fascinated chemists for many decades, this is due to their rich and diverse chemistry, and their medicinal and photochemical properties [1-3]. Flavonoids, are a class of polyphenols obtained through secondary metabolism pathways, that are present in our diet and possess multiple biological activities [4]. The Algar, Flynn and Oyamada reaction is used to synthesize 2-aryl-3-hydroxy-1-benzopyran-4-ones (flavonols) via the alkaline hydrogen peroxide oxidation of 2'-hydroxychalcones (Figure 1), but it can also give other products, that include: 2-aryl-2,3-dihydro-3-hydroxy-1-benzopyran-4-ones (dihydroflavonols) and 2-arylidenebenzofuran-3-ones (aurones) [5,6]. The advantage of this oxidative cyclization method is that hydrogen peroxide is a green reagent that produces water as a product. Unfortunately, the AFO reaction is notorious for moderate yields [7] and thus insights into the mechanism with potential to improve the yields are very welcome.

It was presumed initially that the AFO reaction involved epoxide intermediates, that subsequently underwent intramolecular ring-opening at either the $\alpha$- or $\beta$-positions to afford either flavonols or aurones (Figure 1, b) [8]. However, later Dean and Podimuang on the basis of a number of key studies suggested
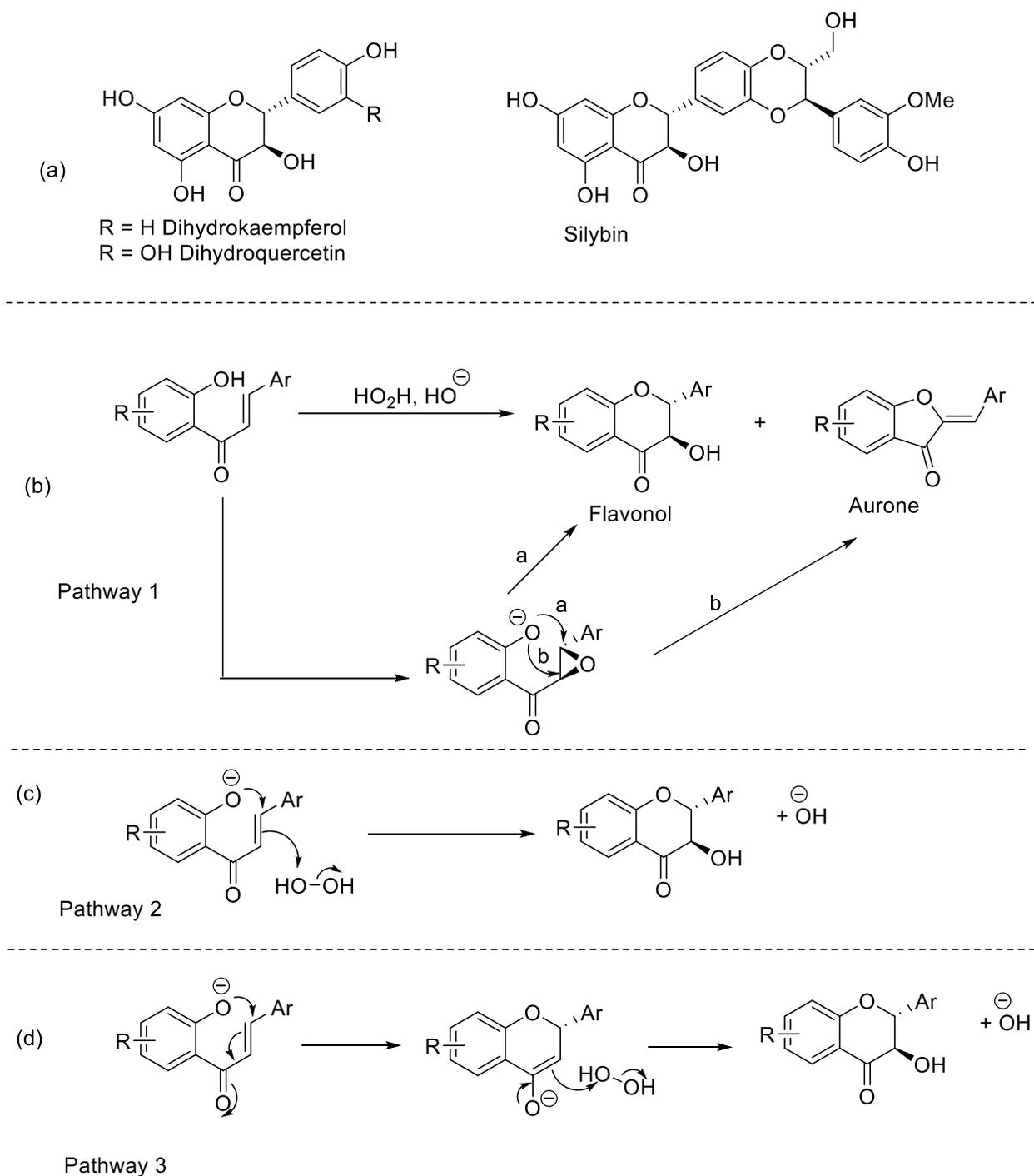
**Figure 1**. (a) Some flavanol containing natural products. (b) The Algar-Flynn-Oyamada reaction, with pathway 1, generation of an epoxide intermediate, (c) pathway 2, the Dean and Podimuang concerted mechanism and (d) pathway 3, the Dean and Podimuang step-wise mechanism. Apart from the compounds shown in Fig. 1 (a), all the compounds described in this paper are racemic mixtures, but only one of the enantiomers is shown.

that epoxides were not intermediates in the formation of flavonols and derivatives, because the strongly alkaline conditions would convert the 2'-hydroxychalcones to their phenolates and due to electrostatic repulsion of the hydroperoxide anion and internal electronic deactivation, epoxidation would be prevented

from occurring [9].  Nonetheless, these authors suggested that in the case of 6'-substituted substrates, the phenolic unit would be forced to become no-longer coplanar with the carbonyl unit, favouring epoxidation of the chalcone, at 0 °C. This would explain the preferential formation of aurones and derivatives under these circumstances. The mechanism fell under intense scrutiny during several years, some questioning the presence of an epoxide intermediate [10,11] and others suggesting the presence of this intermediate under all conditions [12]. Bennett *et al.* provided evidence to support the presence of an epoxide intermediate in the epoxidation of 6'-substituted-2'-hydroxychalcones [13], which addressed the issues previously raised by Philbin's group [10,11]. Furthermore, Gormley and O'Sullivan provided evidence for the intermediacy of epoxides when 2'-tosyloxy-6'-methoxychalcone was transformed to 4-methoxyaurone [14] by treatment of the isolated epoxide with alkali at room temperature, whilst Adams and Main presented further evidence, when 2'-hydroxy-6'-methoxychalcone epoxide was treated with aqueous acetonitrile solutions to afford, 5-methoxyflavonol (β-cyclization product, see (b) Figure 1), aurone, hydrated aurone and benzofuranone resulting from retro-aldol reaction of the latter [15]. Similar to the work of Gormley and O'Sullivan, Burke and O'Sullivan [16] showed the quantitative transformation of 2'-hydroxy-4-methoxychalcone epoxide to *trans*-2,3-dihydro-4'-methoxyflavonol by heating the former in methanol. The selective formation of a flavonol and not an aurone, was most likely due to the close proximity of the 2'-phenolate oxygen with the β-carbon of the epoxide leading to the pyran-4-one ring via a favourable 6-*Exo-Trig* cyclization. Support for this hypothesis comes from earlier conformational, kinetics and mechanistic studies by Adams and Main with analogous systems [15, 17]. Very strong evidence for the generation of an epoxide intermediate with 6'-substituted derivatives was provided by Shen *et al.* who studied a modified AFO reaction on 6'-methoxy-2'-hydroxychalcone using $Na_2CO_3$ as the base, and both the corresponding epoxide and the epoxide derivatives were detected by ^{1}H NMR and LCMS [18].

On the other hand, Schlenoff and co-workers, on the basis of their experiments, asserted that the epoxide intermediate was present under all circumstances [19].  Conclusions obtained upon subjecting some 2'-aminochalcones (the non-substituted entity and 2'-methylaminochalcone) and 2'-methoxychalcone to the AFO conditions, and isolating the corresponding epoxides. However, this was later suggested to be due to the fact that in each case the 2'-substituent ($NH_2$, NHMe and OMe) is much less deactivating than a 2'-oxide unit, probably allowing the epoxidation to proceed [20]. The authors themselves, recognised that the 2-amino group possesses a much lower nucleophilicity than the corresponding OH group.

To date, the only computational study reported for the AFO mechanism is that of Serdiuk *et al.* [21]. These authors conducted low-level semi-empirical calculations (RM1 and PM6 methods) and concluded that in the case of 2'-hydroxychalcones unsubstituted in the 6'-position the pathway involving an epoxide intermediate was more likely that the Dean and Podimuang mechanism. The principal reason, was the very high energy barrier required for the interconversion of the S-*trans* conformation to the S-*cis* conformation, a prerequisite for either of the non-epoxide forming routes (Figure 1 (c) and (d)).

In this paper we report our studies on high level DFT calculations determining the transition state energies for the formation of most of the key intermediates involved in the purported mechanisms in order to understand better the reaction mechanism, and the existence of an epoxide intermediate or not in this reaction. We also studied some alternative conditions for the AFO reaction, albeit with some limited success.

## Results and Discussion

In order to elucidate the mechanism of the Algar–Flynn–Oyamada reaction, on a firmer basis, we conducted a series of high-level computational DFT studies to compare the original epoxide intermediate mechanism (Hypothesis 2) with the non-epoxide involved mechanism of Dean and Podimuang (Hypothesis 1). To evaluate the influence of the presence or absence of a 6'-substituent (the R-group in our discussion) on the reaction kinetics and thermodynamics we carried out our studies with 2'-hydroxychalcone (R = H) and 2'-

hydroxy-6'-methoxychalcone (R = OMe). The effect of the temperature was also evaluated through the calculation of the thermal, entropic and zero-point energy (ZPE) corrections at 0 °C and 25 °C for each transition state structure and related minima (reactant and product).
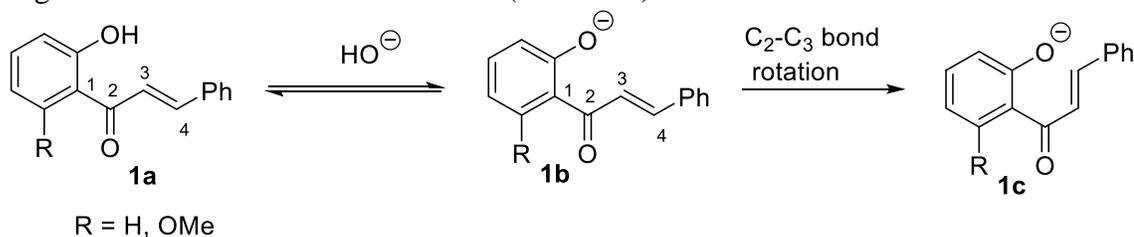
In *hypothesis* 1 -– (Figure 1, pathways 2 and 3) the conversion of the 2'-hydroxychalcone into flavonol starts with the cyclization of 2'-hydroxychalcone anion at the C3 position, with simultaneous nucleophilic attack on the electrophilic oxygen of the hydrogen peroxide molecule at the C2 position to give the flavanol (Figure 1, c). Additionally, the step-wise mechanism involving first the formation of the benzopyran enolate followed by nucleophilic addition at the electrophilic oxygen of the hydrogen peroxide was also evaluated.

In *hypothesis* 2 (Figure 1, b) the 2'-hydroxychalcone is first converted into the chalcone epoxide with the subsequent cyclization of the epoxide, that can occur at either the $C_\beta$ or $C_\alpha$, originating a flavanol or an aurone respectively.

In both tested hypotheses the mechanism starts with the 2'-hydroxychalcone in its deprotonated form. We tried to computationally simulate the 2'-hydroxychalcone deprotonation to quantify the associated energetic cost. The basic pH was simulated through the inclusion of a hydroxide molecule (OH⁻) near the protonated 2´-hydroxyl group of the chalcone. Despite our efforts, we were unable to isolate and identify a transition state structure for this proton transfer, since the proton was spontaneously transferred to the negatively charged hydroxide molecule during the reactant optimization step. This result suggests that in basic media both protonated and deprotonated forms (Scheme 1) may exist in equilibrium, although the deprotonated form is favored.

## Hypothesis 1: Electrophilic Oxidation of the Benzopyran-3-one enolate

In *hypothesis 1* the mechanism starts with the 2'-hydroxychalcone in the **1c** conformation, and, therefore its dihedral angle C1-C2-C3-C4 must rotate ~200° (Scheme 4).



R = H, OMe

**Scheme 1.** Conversion of 2'-hydroxychalcone **1a** to its anion in the S-*trans* conformation **1b** followed by interconversion to the S-*cis* conformation **1c**.

To evaluate the energetic cost associated with this conformational change, we performed a 360° dihedral rotation along the C1-C2-C3-C4 dihedral angle. The energy was calculated for each conformation after each 10° rotation step. The global energetic profile, represented in Figure 2, was obtained by calculating the energy difference (ΔE) between each resulting structure and the departing structure **1b**.
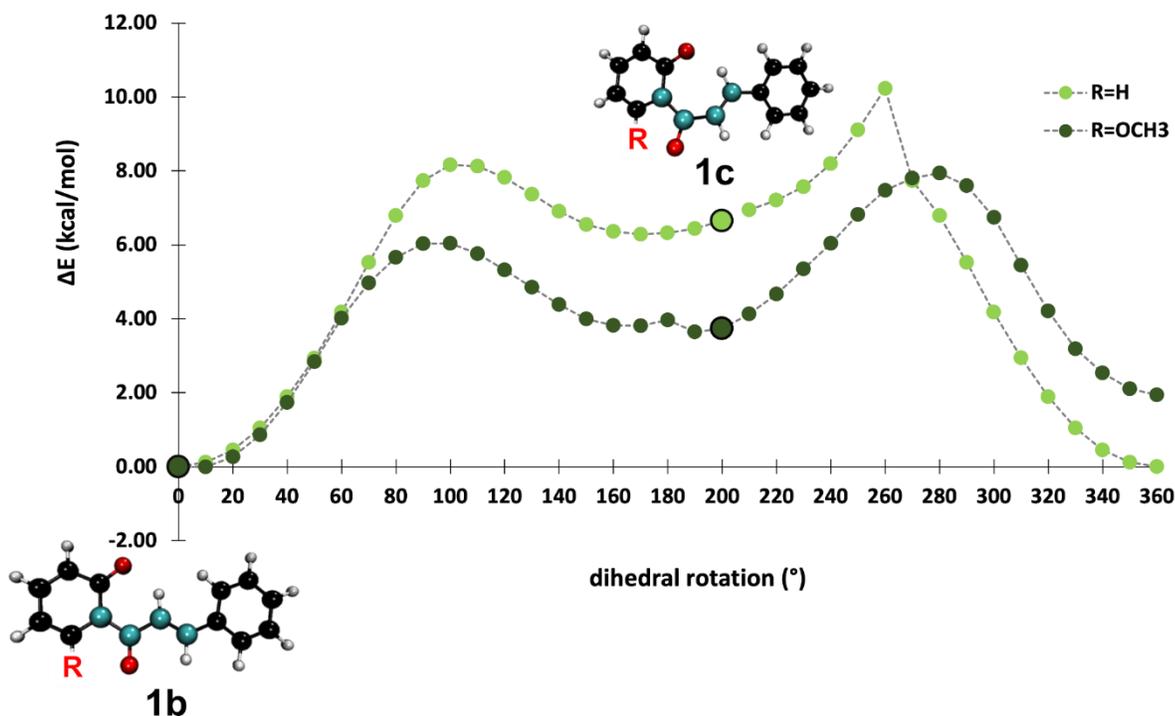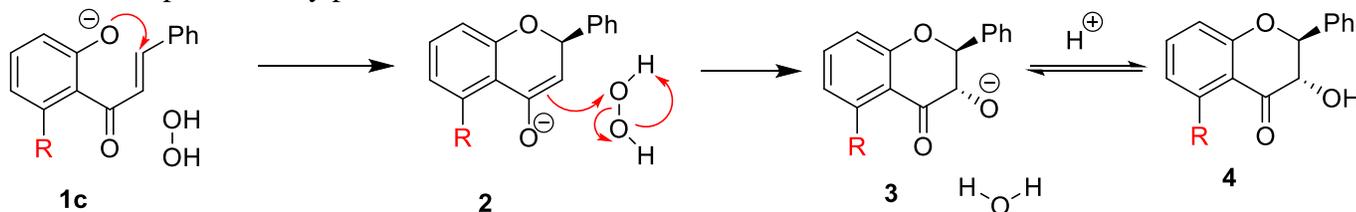
**Figure 2**. Schematic representation of the conversion of conformer **1b** to conformer **1c** by rotation about the C1-C2-C3-C4 dihedral angle (colored in cyan) 200°. Both **1b** and **1c** are represented as a CPK structure from VMD ..

Surprisingly it was observed that the rotation by 200° about the C1-C2-C3-C4 dihedral angle had a higher energy cost (*aprox.* 6 kcal/mol) for the unsubstituted 2'-hydroxychalcone anion than for the 6'-methoxy substituted analogue (Figure 2). This might be due to a stabilization effect from the methoxyl unit. After the C1-C2-C3-C4 dihedral rotation, the conversion of the 2'-hydroxychalcone **1c** into a flavannol oxy-anion **3** requires two sequential steps that are schematically represented in scheme 5. In the first step the negatively charged oxygen will attack C3 leading to the cyclization of the chalcone anion to form the benzopyranone enolate **2**. In the second step the enolate will attack the most electrophilic oxygen of the hydrogen peroxide to introduce the oxygen at C2 forming the flavanol oxy-anion **3**, that can then undergo protonation to give the flavanol product **4** by protonation from water.



**Scheme 2.** Proposed mechanism for the stepwise conversion of the 2'-hydroxychalcone oxy-anion **1c** into flavanol **4,** via intermediates **2** and **3** (R = H, OMe).

The obtained free energies of all steps of the mechanism are summarized in Table 1.

**Table 1.** Activation ($\Delta G^\ddagger$) and reaction free energies ($DG_r$) obtained for each step of the mechanism tested in Hypothesis 1 – conversion of **1c** to **2**.

| | -R | $\Delta G^\ddagger$ (kcal/mol) | | $\Delta G_r$ (kcal/mol) | |
|---|---|---|---|---|---|
| | | T=25°C | T=0°C | T=25°C | T=0°C |
| Step 1 | -H | 11.4 | 11.3 | -4.8 | -4.9 |
| | -OCH$_3$ | 17.4 | 17.1 | 4.6 | 4.2 |
| Step 2 | -H | 25.7 | 25.7 | -64.0 | -63.9 |
| | -OCH$_3$ | 22.5 | 22.7 | -61.2 | -61.2 |

As discussed above (Scheme 2), in order to evaluate if the reaction occurred in a concerted pathway, we tested the simultaneous attack of the negatively charged oxygen at C3 with simultaneous nucleophilic attack at the most electrophilic oxygen of the hydrogen peroxide (Figure 1(c,) pathway 2). In all our attempts to simulate this mechanism we only observed (R = H, OMe) the cyclization of the 2'-hydroxychalcone anion to give the benzopyranone enolate **2**. This result seemed to rule out the concerted mechanism for formation of flavanol **4** from 2'-hydroxychalcone **1a** during the AFO reaction (Figure 1 (c), pathway 2). This is in conformity with previous conclusions of Serdiuk *et al.* [21] who ruled out this mechanistic hypothesis.

**Dihedral rotation**

The 2'-hydroxychalcone anion **1b**, independent of the R group, has a C1-C2-C3-C4 dihedral angle of 180°. Its conversion into conformation **1c** requires a C1-C2-C3-C4 dihedral rotation of 199.77° (R=H) (**1c** dihedral angle=19.77°) and a rotation of 203.11° for R=OCH$_3$ (**1c** dihedral angle=23.11°).
The conformers **1b** and **1c** were optimized and the Gibbs free energy difference between the **1c** and **1b** calculated. The results showed that for **1b** (R=H), the C1-C2-C3-C4 dihedral rotation, requires 6.3 kcal/mol and it is not affected by the temperature. In the case of **1b** (R=OMe) the same rotation requires only 3.0 kcal/mol at 25°C and 2.5 kcal /mol at 0°C.
These results indicate that:
(1) the R group influences the energetic cost of the C1-C2-C3-C4 dihedral rotation, that is lower for **1b** (R=H).
(2) the temperature only had a slight effect on the dihedral rotation of **1b** (R=OCH$_3$) whose rotation is energetically favored (<0.5 kcal/mol) at lower temperature.

**Step 1**

The analysis of the reaction free energies of step 1 (Table 1) shows that the replacement of the 6'-H by a 6'-OMe affects both the kinetics and the thermodynamics of the reaction. The cyclization of the chalcone anion **1c** (R=OMe) requires an extra 6 kcal/mol of energy to occur when compared with **1c** (R=H). Additionally, this reaction is exergonic by 4.8 kcal/mol for **1c** (R=H) as compared to **1c** (R=OMe) which is endergonic by 4.6 kcal/mol. This suggests that the R group has a strong effect on the stability of the benzopyran-3-one enolate **2** (Scheme 2): the benzopyran-3-one enolate anion **2** (R=H) is stable ($\Delta G_r$ =-4.8 kcal/mol, @25 ºC), whilst the benzopyran-3-one enolate **2** (R=OMe) is unstable ($\Delta G_r$ =+4.6 kcal/mol @25 ºC) and its reversion to the departing 2'-hydroxychalcone oxy-anion **1c** only requires 12.8 kcal/mol to occur as opposed to 16.2 kcal/mol for **2** (R=H).

**Step 2**

The analysis of the reaction free energies of step 2 (Table 1) shows that, analogous to what has been observed for step 1, the replacement of an -H by an -OMe in the 6-position affects both the kinetics and the thermodynamics of the reaction. In this reaction the activation free energy is 3.2 kcal/mol lower for **2** (R = OMe) when compared to **2** (R=H) (22.5 kcal/mol vs. 25.7 kcal/mol), but the reaction with **2** (R=H) is more exergonic by 2.8 kcal/mol (-64 kcal/mol vs. -61.2 kcal/mol). This result suggests that the presence of a 6'-methoxyl group favors the reaction kinetics of this reaction step, but penalizes the reaction thermodynamics.

**Energetic profile**

The overlap of the energetic profiles of the mechanisms tested in hypothesis 1 is represented in Figure 3 and it shows that:
(1) The rate limiting step of both reactions (R=H and R=OMe) is the nucleophilic attack of the enolate on the electrophilic oxygen of hydrogen peroxide at the C3 carbon atom.
(2) The R group affects the overall kinetics and thermodynamics of the reaction: when R=H the reaction is more exogonic, i.e. the benzopyran-3-one enolate **2** (R=H) is more stable than when R=OMe.
2) The reverse reactions require >89 kcal/mol to occur which suggests that both benzopyran-3-one enolates are very stable and that the reactions are irreversible.
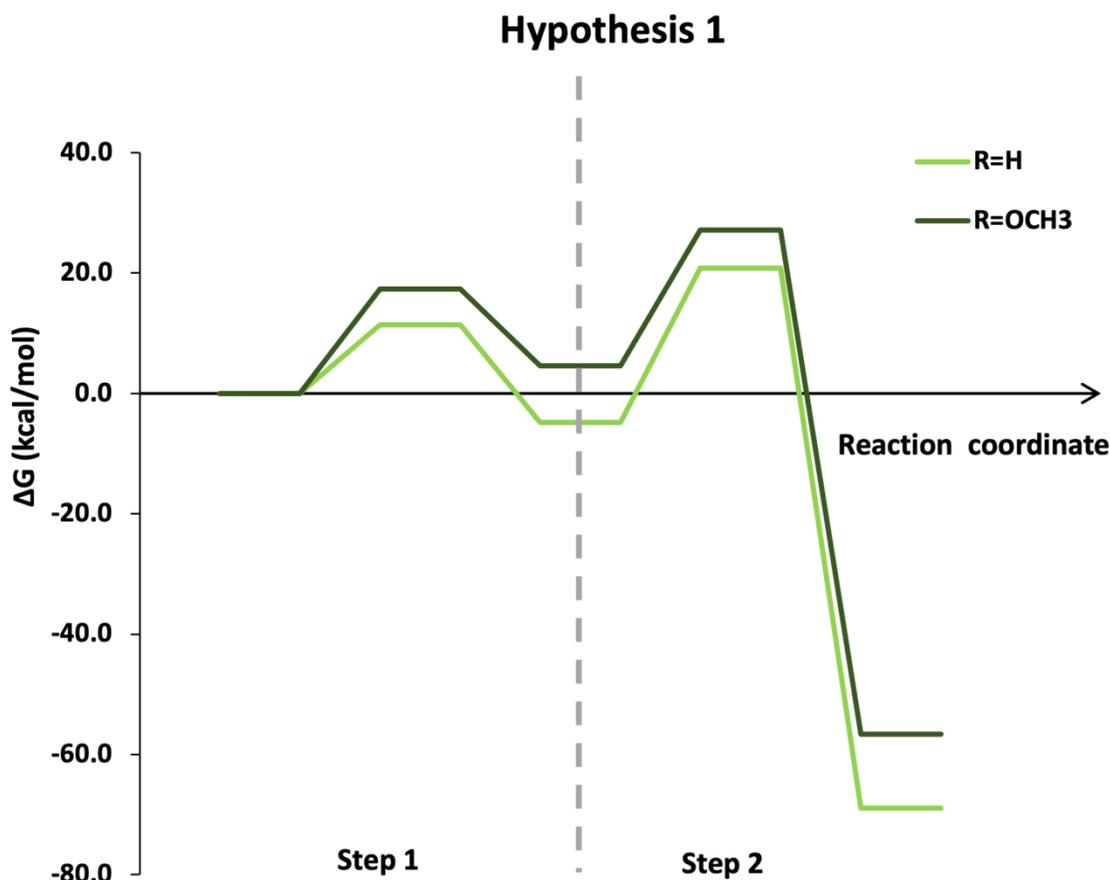


**Figure 3**. Energetic profile of the stepwise conversion of the 2'-hydroxychalcone **1a** (R = H, OMe) into the flavanol oxy-anion **3** according to *hypothesis* 1.

In the case of hypothesis 1, the kinetic profile for R = H was more favorable than for R = OMe, as was the thermodynamics. Which agrees with the postulate of Dean and Podimuang [9].

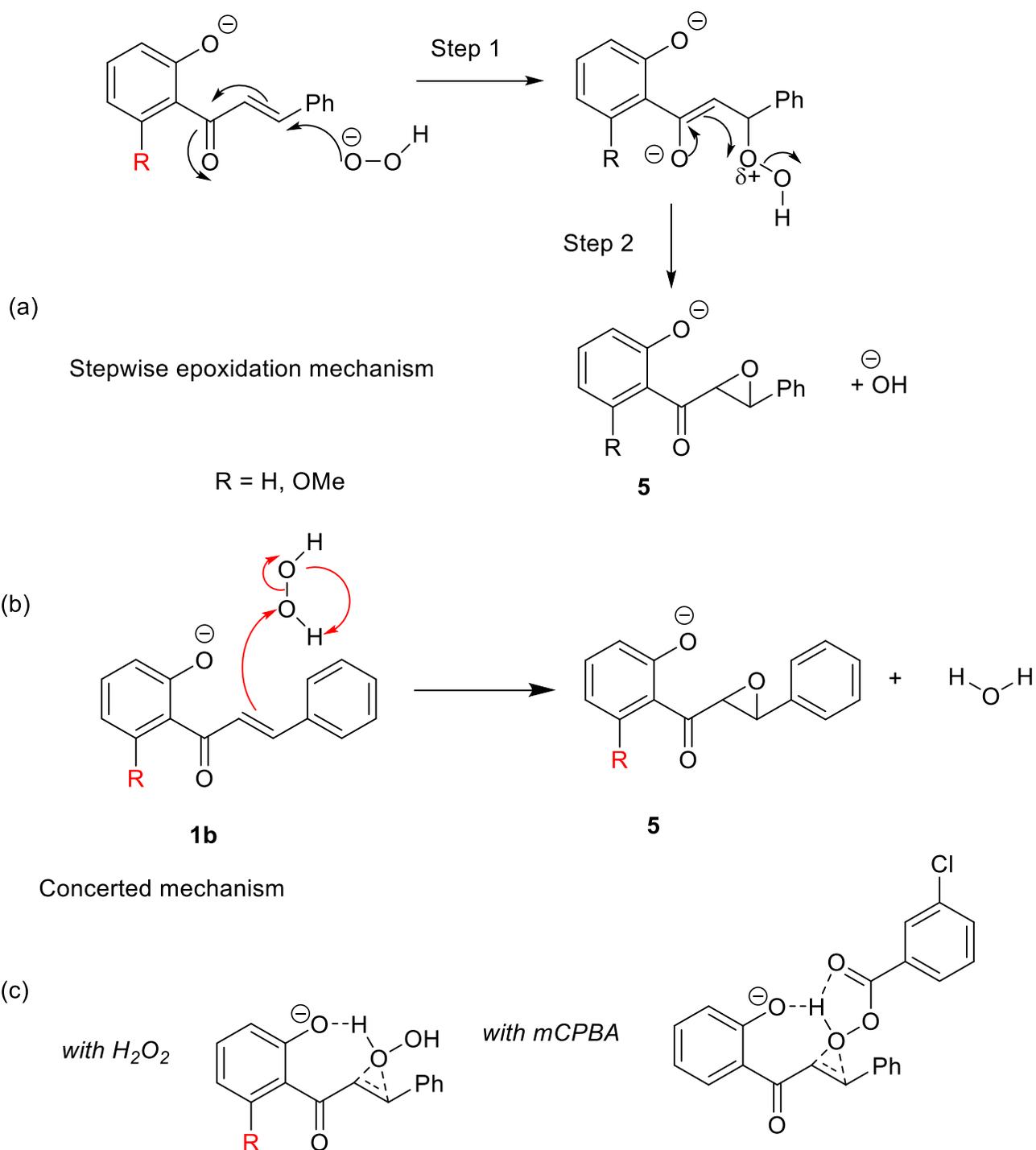**Hypothesis 2: Epoxide intermediate pathway**

The second hypothesis tested also requires two sequential steps (Figure 1, b), but it follows a completely different pathway, i.e. it involves the presence of an epoxide intermediate. The proposed mechanism starts with the nucleophilic attack of the peroxide's oxygen to the C3 carbon of the deprotonated 2'-hydroxychalcone with its C1-C2-C3-C4 dihedral angle in its more stable conformation **1b** (Scheme 3(a)). The product of this reaction is a chalcone epoxide and a hydroxide molecule. Amazingly, our calculations failed to afford the epoxide intermediate (for both R = H and OMe), and indicated the concerted electrophilic mechanism shown in Scheme 3(b). This was an unexpected finding, as hydrogen peroxide type epoxidations with chalcones are nucleophilic taking place according to the mechanism originally proposed by Bunton and Minkoff [22]. However, this is not a normal enone system, and as proposed by Dean and Podimuang the enone system is deactivated for normal 1,4-conjugate addition by the peroxide anion, and thus the alternative electrophilic epoxidation mechanism is a viable alternative. Indeed, there have been reports of the electrophilic epoxidation of alkenes via stabilizing hydrogen bonding networks.For instance Jacobs and coworkers demonstrated the power of phenol as an activating agent to facilitate the oxygen-atom transfer [23] and later De Vos and coworkers showed that the solvent can also active the oxygen-atom transfer in a particular epoxidation reaction [24]. Sulfonic acids have also been shown to catalyze these reactions [25]. These observations have been incorporated into the putative working model shown in Scheme 3 (c).

Finally, another piece of evidence that supports this conjecture, was the observation by Dean and Podimuang of a slow general oxidation of 4'-hydroxychalcone [9], a result that was later puzzling for Schlenoff and coworkers [19].
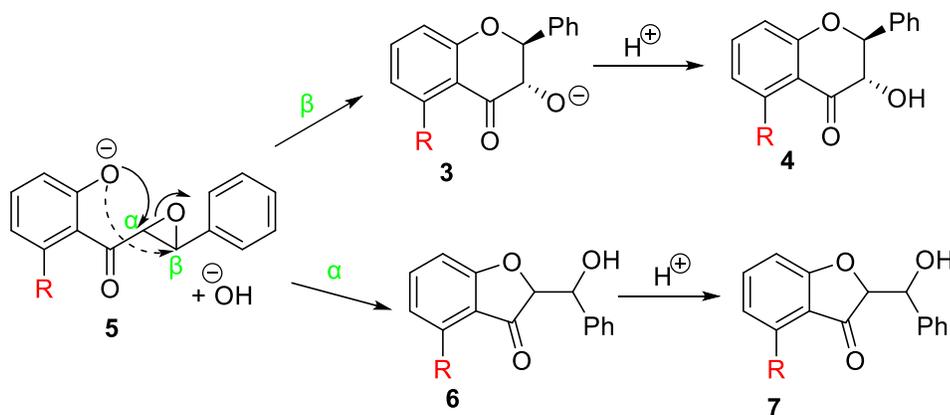
The question then arises why does this mechanism of electrophilic epoxidation operate for both R=H and R = OMe (normally reserved for unfunctionalized alkenes). This maybe a consequence of the reduction of the carbonyl electrophilicity via inductive electron transfer from the 2'-oxy anion moiety.
In the second step of the mechanism there is an attack by the 2'-phenoxide oxygen on the oxirane ring leading to either the benzofuran-3-one intermediate **6** (attack at the α-carbon) and/or the flavanol oxide **3** (attack at the β-carbon) (Scheme 4).  Protonation in each case leads to the auronol **7** or the flavanol **4**.

The obtained free energies of all reaction steps are summarized in Table 2.

**Scheme 3. (a)** Proposed mechanism for step 1 of *hypothesis* 2 (R = H, OMe). Nucleophilic epoxidation of 2'-hydroxychalcone oxide **1a**. **(b)** Electrophilic epoxidation mechanism indicated by the DFT calculations. **(c)** Putative hydrogen-bonding model between the 2-oxy unit and $H_2O_2$, and with mCPBA with "butterfly" transition state.

10

**Scheme 4.** Proposed mechanisms for step 2 of hypothesis 2. Transformation of **5** into **4** and **7**, respectively.

**Table 2**. Activation ($\Delta G^{\ddagger}$) and reaction free energies ($\Delta G_r$) obtained for each step of the mechanism tested in Hypothesis 2 – transforming

| | -R | $\Delta G^{\ddagger}$ (kcal/mol) | | $\Delta G_r$ (Kcal/mol) | |
|---|---|---|---|---|---|
| | | T=25°C | T=0°C | T=25°C | T=0°C |
| **Step 1** | -H | 43.4 | 43.2 | -48.2 | -48.5 |
| | -OCH$_3$ | 42.8 | 42.6 | -48.7 | -49.0 |
| **Step 2 (C$_\alpha$)** | -H | 20.5 | 20.4 | -3.7 | -3.9 |
| | -OCH$_3$ | 18.3 | 18.2 | -6.5 | -6.7 |
| **Step 2 (C$_\beta$)** | -H | 20.1 | 20.0 | -4.1 | -4.2 |
| | -OCH$_3$ | 21.5 | 21.3 | -6.0 | -6.1 |

- **Analysis of the effect of R=H vs R=OMe**

**Step 1**

The analysis of the activation and reaction free energies of the reaction (Table 1) indicated that the replacement of a -H by an OMe group did not influence neither the kinetics nor the thermodynamics of the first step of the mechanism (Scheme 3). This step has a mean activation free energy of 43.1 ±0.4 kcal/mol and is exergonic to a mean value of 48.5±0.4 kcal/mol. The analysis of the energetic profile of the reaction (Figure 3) indicates that the reverse reaction would require ~91kcal/mol to occur, suggesting that the generated chalcone epoxides **5** are very stable products and therefore their reconversion to the departing 2'-hydroxychalcone **1b** is unlikely to occur.

**Step 2**

Regarding the second step of the mechanism, the analysis of the calculated free energies shows that the replacement of an -H by a -OMe group affects both the kinetic and thermodynamic properties of the reaction

11

in different ways. Moreover, whilst in the case of the chalcone epoxide anion **5** (R=H) there are no significative differences in both the activation free energy and reaction free energy of the reactions for the attack on the $C_\beta$ or the $C_\alpha$, in the chalcone epoxide, in the case of the other epoxide anion (R =OMe), the attack on the $C_\alpha$ is kinetically favored by 3.2 kcal/mol (leading to the β-hydroxybenzofuran-3-one **7** over the attack to the $C_\beta$ (18.3 kcal/mol vs. 21.5 kcal/mol). This is probably accounted for by repulsion between the carbonyl unit and the 6'-methoxy group as discussed previously in the literature, , [9,13,16]. Examination of the calculated transition state structure for the $C_\beta$ attack, showed that the methoxyl oxygen is 0.13 Å closer to the carbonyl group than in the transition state structure of the $C_\alpha$ attack (2.65 Å vs 2.78 Å). The increase in the intensity of the stereochemical repulsions in the $C_\beta$ attack transition state structure may contribute to the 3.2 kcal/mol increase in the activation free energy of the reaction.

The same stereochemical effect may explain the increase of 1.4 kcal/mol in the activation free energy for the $C_\beta$ attack when the -H is replaced by an -OMe.

Moreover, there were no differences in the reaction free energies for the $C_\beta$ and $C_\alpha$ reactions when R=OMe (Table 2 -6.5 and 6 at 25 $^\circ$C and -6.7 and -6.1 $^\circ$C at 0 $^\circ$C), but however, it has been observed that the replacement of a -H for an -OMe positively affects the thermodynamics of both $C_\alpha$ and $C_\beta$ attack by lowering the reaction free energy by ~2.3 kcal/mol (-3.9 ± 0.2 kcal/mol vs -6.1 ± 0.4 kcal/mol) in the case of the $C_\beta$ attack. This difference may be due to the electronic properties of the methoxyl group that can behave as an electron-withdrawing group and stabilize the negative charge of the products.

**Energetic profile**

The overall situation of the energetic profiles of the reactions tested in hypothesis 2 is represented in Figure 4 and it shows that:

(1) Independent of the type of R group, the reactions have similar energetic profiles with slight differences in the kinetics and thermodynamics of the second step, as already discussed.
(2) The reactions are all exergonic at ~50 kcal/mol suggesting that they are irreversible and that the resulting flavonol oxy-anion **5** and aurone oxy-anion **6** products are very stable.
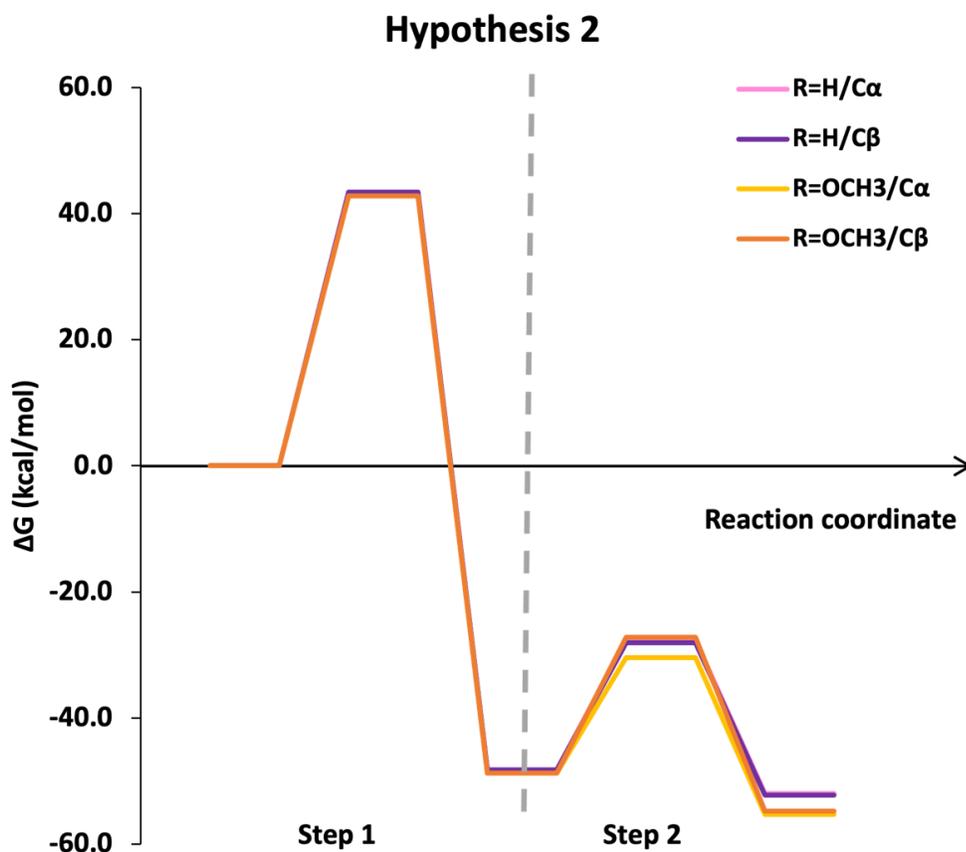
**Figure 4.** Energetic profile of the conversion of the 2-hydroxychalcone anion **1b** into the flavonol oxy-anion **3** and aurone oxy-anion **6** according to hypothesis 2.

- **Hypothesis 1 vs Hypothesis 2 (R = H)**

The overlap of the energetic profiles of the two studied mechanisms that originates the flavonol oxy-anion **5** (R=H) (hypothesis 1 vs. hypothesis 2; $C_\beta$) is represented in Figure 5. This analysis firmly suggests that the mechanism described in hypothesis 1 is kinetically and thermodynamically more favorable that the one described in hypothesis 2.
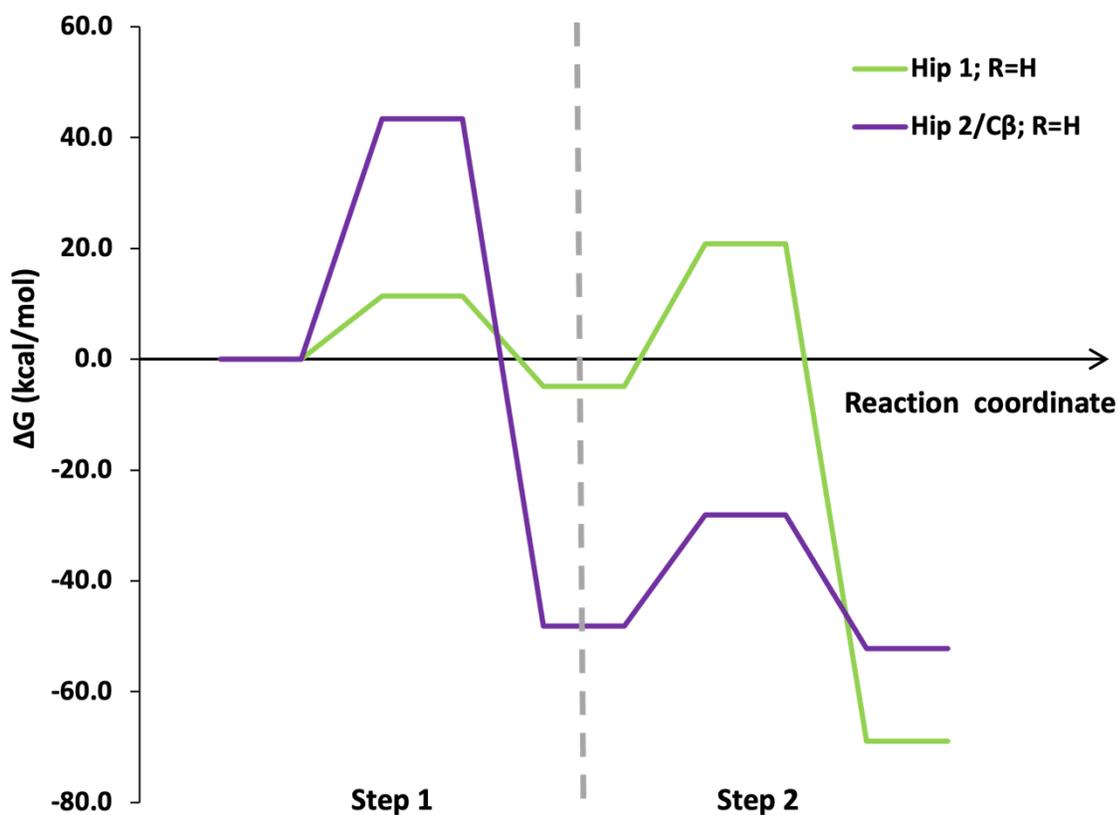
**Figure 5**. Superimposition of the energetic profiles obtained for the conversion of the 2'-hydroxychalcone **1b** to the flavonol oxyanion **3b** according to *hypothesis* 1 and hypothesis 2 (R=H; $C_\beta$).

- **Hypothesis 1 vs Hypothesis 2 (R = OMe)**

The overlap of the energetic profiles of the two studied mechanisms that originates the flavonol oxyanion **5** (R=OMe) (hypothesis 1 vs. hypothesis 2; $C_\beta$) is represented in Figure 6. This analysis firmly suggests that the mechanism described in hypothesis 1 is kinetically more favorable that the one described in hypothesis 2, however, thermodynamically both mechanisms are quite similar.
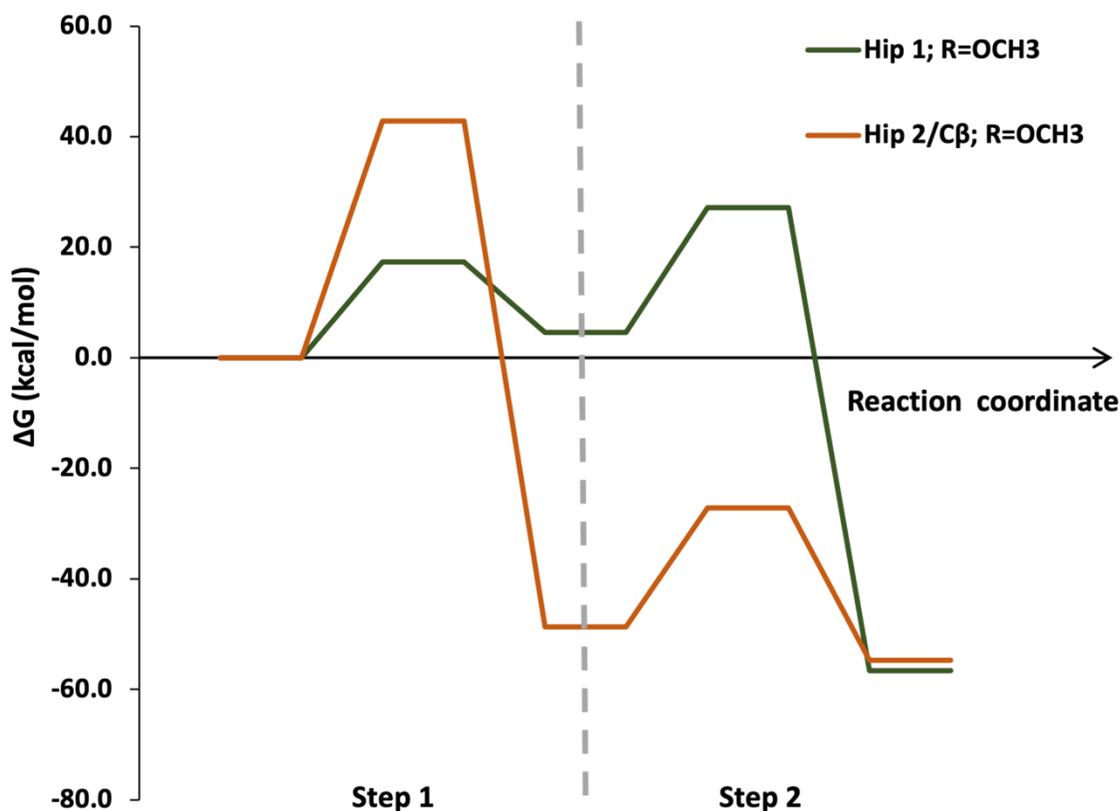
**Figure 6**. Superimposition of the energetic profiles obtained for the conversion of the 2'-hydroxychalcone **1b** to the flavonol oxyanion **3b** according to *hypothesis* 1 and *hypothesis* 2 (R=OMe; attack at $C_\beta$).

### The effect of Temperature (0 °C vs. 25 °C)

The analysis of the results summarized in Table 1 and Table 2 show that the variations in free energies when the reaction is simulated at 0 °C or at 25 °C, are in the range 0.0-0.4 kcal/mol, or in other words there is little effect of temperature on the reaction result.

Our results clearly show that when R = H, *hypothesis* 1 is favored, which makes sense considering the arguments given by Dean and Podimuang [9]. When R = OMe, the reaction kinetics favor *hypothesis* 1, but the thermodynamics favour both mechanisms.

### The AFO reaction with mCPBA: A simple modification

In an attempt to gain insight into the mechanism of the AFO, reaction and to gain further support the Dean and Podimuang mechanism, we studied a variant of this reaction with *m*-chloroperbenzoic acid (mCPBA) instead of hydrogen peroxide (Figure 1 (c), (d)). Considering the structure of this oxidant (with a good electron withdrawing group), it was anticipated that the AFO reaction should show better reaction kinetics. Some experiments with **1a** were conducted with mCPBA and different bases (Figure 7). In the case of the

first reaction (Figure 6, (a)) it was carried out 0 °C for 10 min, then room temperature 20 min and afforded a mixture of the 3-hydroxyflavanone **4** (7% crystallized) and flavanone **8** (60% isolated yield). Suspecting that **8** was the result of protonation of the benzopyranone (flavanone) enolate **2**, we allowed the reaction to run longer (Figure 6, (b)), and it gave the flavonol **9** (15% crystallized). TLC analysis of the filtrate after recrystallization revealed a mixture of **1a** and **8**, which was a strong indication that the extra reaction time led to oxidation of the 3-hydroxyflavanone **4** to flavonol **9**. The fact that both substrate **1a** and flavanone **8** were recovered was a clear indication that this modification failed to be improvement on the original method. Assuming that the reaction pH had a negative effect on the reaction, probably deprotonating the mCPBA we substituted the hydroxide with the weaker piperidine base, and left the reaction for longer (constantly monitoring by TLC), unfortunately the substrate was recuperated in 66% yield, including flavanone **8** (16%) and flavonol **9** (3%). All these results clearly indicate that cyclization is taking place to give the flavanone enolate (Scheme 2, **2** R = H), which appears to be protonated by the mCPBA (which is always in excess) or during work up, instead of being oxidized. Despite this occurrence, these results offer support to the Dean and Podimuang hypothesis, or the step-wise mechanism (Figure 1(d)).
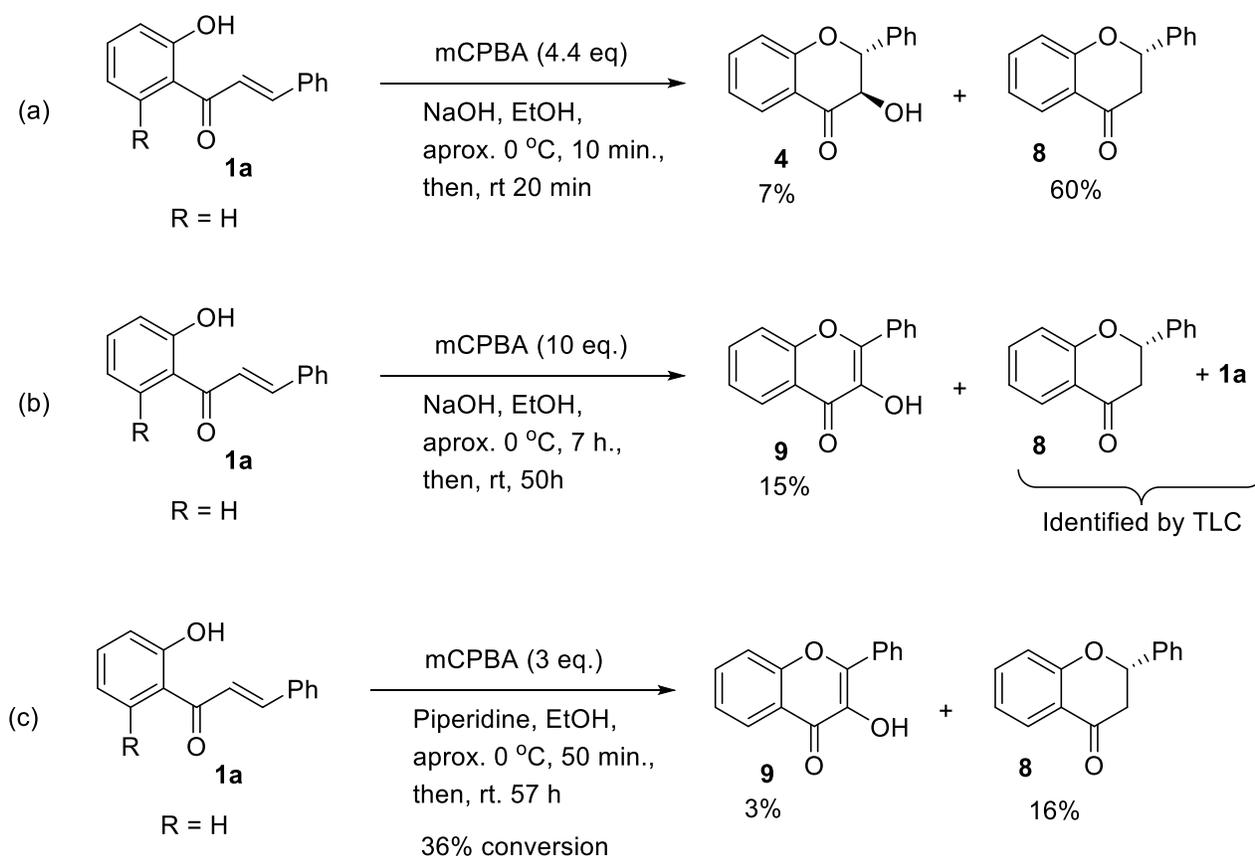


**Figure 7.** (a) to (c) show different reaction conditions in an attempt to optimize the AFO reaction using mCPBA instead of $H_2O_2$.

## Conclusions

A detailed computational study was carried out using 2'-hydroxychalcone **1a** (R = H) and 2'-hydroxy-6'-methoxychalcone **1a** (R = OMe) as the model substrates. Two mechanistic pathways were studied by DFT

16

with the B3LYP functional, incorporating Grimme's empirical dispersion corrections (GD3), Becke-Johnson damping (BJ) and the 6-31G(d,p) basis set (see references below); *hypothesis* 1, the Dean and Podimuang, non-expoxide pathway and the epoxide intermediate pathway, *hypothesis* 2. Our calculations showed that in the case of *hypothesis* 1, the most favorable outcome in terms of kinetics and thermodynamics was observed when R = H, in conformity with the original hypothesis of Dean and Podimuang [9]. However, in the case of *hypothesis* 2, once again the best kinetic profile was observed when R = H, but both substrate types (R = H and OMe) gave comparable thermodynamic pathways. This seems to indicate that in the case of the former substrates the Dean and Podimuang operates and in the case of the latter, the two mechanisms may be operating simultaneously, but with a better reaction rate in the case of the Dean and Podimuang mechanism.

Strangely, and a point that previously has never been raised, the classical Bunton and Minkoff peroxide enone addition product of chalcone oxide **1b** (R = H, OMe) could not be computed (was not identified in the calculation), and an electrophilic addition on the peroxide molecule was computed instead. Also, some changes to the usual AFO conditions using mCPBA lent some support to the Dean and Podimuang hypothesis. We plan to carry out further computational studies on this mechanism to understand fully the intricacies of this pathway, and if it competes with the Dean and Podimuang mechanism. A "butterfly" mechanism similar to that shown in Figure 3 (c) is possible, but perhaps the kinetics for ring closure to the enolate **2** is faster than the electrophilic epoxidation via the mCPBA due to perhaps a higher reaction activation energy, which maybe a consequence of steric hindrance. This is something we wish to explore in the near future.

## Experimental

## Chemical Synthesis: General

Reagents were obtained from Sigma Aldrich and Alfa Aesar (formally Lancaster )and were used as received. The solvents used were dried using standard laboratory techniques. Column chromatography was carried out on silica gel (Merck Kieselgel 60) and for flash chromatography (Merck Kieselgel 60, 40–63 μm). Thin-layer chromatography (TLC) was carried out on aluminium-backed Kieselgel 60 F254 plates (Merck). Preparative layer chromatography (PLC) was preformed using Merck Kieselgel PF254+336. Plates were visualized by UV light. Melting points (m.p.) were determined with a Reichert-Jung hot stage apparatus and are uncorrected. NMR spectra were recorded with a Jeol JNM-GX-270 spectrometer with a broadband probe. Chemical shifts are quoted in parts per million (ppm) relative to 0.0 ppm of TMS (internal standard). Coupling constants (*J*) are reported in Hz and refer to apparent peak multiplicities. Splitting patterns are reported as s, singlet; d, doublet; dd, double of doublets, t, triplet; m, multiplet; br, broad.
The mCPBA used in the AFO reactionsn was concentrated by drying under vaccum (@ 0.1 Torr) for 10 days, and then the concentration determined iodometrically [26].

*Synthesis of 2,3-Dihydro-2-phenyl-4H-1-benzopyran-4-one (Flavanone)* **8**

## Method 1

*m*-Chloroperbenzoic acid (mCPBA) (3 g, 9.6 mmol, 55%) was added in portions to a stirred solution of 2'-hydroxychalcone **1a** (R = H) (0.5 g, 2.2 mol) in an aqueous sodium hydroxide (5%, 10 mL)-ethanol (30 mL) solution at -5 °C. After 10 min. the reaction mixture was allowed to warm to room temperature and stirred for a further 20 min. The reaction was quenched by the addition of ice-cold water (20 mL). After extraction with $Et_2O$ (2 x 30 mL) the combined extracts were washed with aqueous sodium thiosulphate (5%, 60 mL), aqueous sodium bicarbonate (10%, 3 x 40 mL), brine (40 mL), dried with anhydrous $CaSO_4$

and evaporated to dryness to furnish a pale-yellow oily residue. Purification by column chromatography on SiO$_2$ (DCM/Petroleum spirits 60-80 $^o$C; 8.5/1.5) afforded 2 fractions, listed in order of increasing polarity.

*Fraction 1*

Furnished the *title compound* **8** (0.3 g, 60%) as a white solid, which crystallized from ethanol as plates, m.p. 75-76 $^o$C (lit. 76 $^o$C [27]).

*Fraction 2*

Furnished *trans*-2,3-dihydro-3-hydroxy-2-phenyl-4*H*-1-benzopyran-4-one (Flavanol) **4** (0.0353 g, 7%) as a white solid which crystallized from benzene-petroleum spirits (60-80 $^o$C) as needles, m.p. 176-178 $^o$C (lit. 178 $^o$C [28]).

## Method 2

Piperidine (10 mL, 50.5 mmol) was added to a solution of 2'-hydroxychalcone **1a** (R = H) (1 g, 4.4 mol) in EtOH (5 mL) and briefly stirred at room temperature. It was then lowered to 0 $^o$C and a solution of mCPBA (65%, 2.82 g, 13.2 mmol)) in EtOH (10 mL) was added dropwise. After stirring at this temperature for 50 min. the reaction mixture was warmed to room temperature and stirred for a further 57 h. Water (50 mL) was added and the mixture extracted with diethyl ether (2 x 50 mL), and the combined extracts were washed with aqueous sodium thiosulphate (10%, 90 mL), aqueous sodium bicarbonate (10%, 3 x 40 mL), brine (2 x 70 mL), dried with anhydrous Na$_2$SO$_4$ and evaporated to dryness to furnish an orange syrupy residue. Purification by column chromatography on SiO$_2$ (n-Hexane/EtOAc) afforded 3 fractions, listed in order of increasing polarity.

*Fraction 1*

Gave the starting chalcone compound **1a** as a yellow solid (0.66 g, 66%), which crystallized from EtOH as yellow needles, m.p. 87-89 $^o$C (lit. 88-89 $^o$C [29]).

*Fraction 2*

Furnished flavanone **8** (0.16 g, 16%), which crystallized from EtOH as needles, m.p. 75-77 $^o$C (lit. 76 $^o$C [27]).

*Fraction 3*

Afforded 3-Hydroxy-2-phenyl-4*H*-1-benzopyran-4-one (Flavonol) **9** (0.03 g, 3%) as a pale green solid, which crystallized from ethanol as needles, m.p. 168-170 $^o$C (lit. m.p. 170 $^o$C [30]).

*Synthesis of 3-Hydroxy-2-phenyl-4H-1-benzopyran-4-one* (*Flavonol*) **9**

Aqueous sodium hydroxide (1.4 mL, 5%), was added to a stirred solution of 2'-hydroxychalcone **1a** (R = H) (0.1 g, 4.4 mmol) in ethanol (20 mL) at 0 $^o$C. This was followed by the addition of a solution of mCPBA (50%, 1.38 g, 0.4 mmol) in ethanol (20 mL) over a period of 30 min. The reaction mixture was stirred for a further 50 h. The solvent was removed by evaporation to afford a white residue, which was extracted many times with Et$_2$O (3 x 25 mL). The organic extracts were washed with sodium thiosulphate (10%, 3 x 50 mL), aqueous sodium bicarbonate (10%, 4 x 50 mL) and brine (30 mL). The organic extracts were then dried with anhydrous MgSO$_4$, filtered and the solvent evaporated to afford a yellow solid. Recrystallization

from Et₂O gave the *title compound* **9** (0,153 g, 15%) as needles m.p. 168-169 ºC (lit. m.p. 170 ºC [30]). TLC analysis of the filtrate showed the presence of starting material **1a** and flavanone **8**.


**Computational Studies**

The structures of the reactant molecules were draw with GaussView 5.0.

The geometry optimizations and the search for stationary points were performed using the Gaussian 16 program, by applying density functional theory [31] with the B3LYP functional [32,33]), Grimme's empirical dispersion corrections (GD3) [34], Becke-Johnson damping (BJ) [35] and the 6-31G(d,p) basis set. All the geometry optimizations and the stationary points were obtained with standard Gaussian convergence criteria.

To simulate the solvent used experimentally (> x% water) all calculations were performed in a conductor-like polarizable continuum model obtained through the integral equation formalism variant (IEF-PCM) [36] as implemented in Gaussian 16.

The atomic charge distributions were calculated at the B3LYP level of theory, employing a Mulliken population analysis, using the 6-31G(d,p) basis set.

The study of the different reaction hypotheses started with unidimensional scans along the reaction coordinate of interest. The putative transition state structures suggested by each scan, corresponding to the point of higher energy, were verified by vibrational frequency calculations. The structures with a single imaginary frequency assigned to the correct transition vector were confirmed as transition state (TS) structures and posteriorly optimized and characterized. The minima (reactant and product) associated with each calculated TS structure were determined through intrinsic reaction coordinate (IRC) calculations. The obtained structures were submitted to a final geometry optimization and its nature was confirmed through vibrational frequency calculations that showed the inexistence of imaginary frequencies. During the vibrational frequency calculations, the ZPE, thermal, and entropic energy corrections were estimated at 298.15 K and 273.15 K and 1.0 bar for each TS and related minima structures.

The activation Gibbs free energies of each reaction were obtained by calculating the difference between the Gibbs free energies of the TS and reactant. The reaction Gibbs free energies were obtained by calculating the difference between the Gibbs free energies of each product and corresponding reactant.

The final energies were obtained by adding the ZPE, thermal, and entropic energy corrections, previously calculated with the B3LYP functional, to the energy obtained by single point calculations for each TS, reactant, and product structure using the domain-based local pair natural orbital (DLPNO) coupled-cluster single-, double-, and perturbative triple-excitations (CCSD(T)) theory level in the complete basis set (CBS) method [37-39]. The solvent effects (water) were included using the Conductor-like Polarizable Continuum Model (CPCM) as implemented in ORCA software. The single point calculations procedure was accomplished using the ORCA software (version 5.0.3).

# References

1. Santos, C.M.M, and Silva, A.M.S. *Adv. Heter. Chem.*, **2022**, 138, 159-241. https://doi.org/10.1016/bs.aihch.2022.02.001

2. Pereira, A.M., Cidade, H., Tiritan, M.E., *Molecules*, **2023**, 28, 426. https://doi.org/10.3390/molecules28010426.

3. Formosinho, S.J., Arnaut, L.G. *J. Photochem. Photobiol. A.* **1993**, 75, 1-20. https://doi.org/10.1016/1010-6030(93)80157-5

4. Li, J.; Sun, M.; Cui, X.; Li, C. Protective Effects of Flavonoids against Alzheimer's Disease: Pathological Hypothesis, Potential Targets, and Structure–Activity Relationship. *Int. J. Mol. Sci.* **2022**, *23*, 10020. https://doi.org/10.3390/ijms231710020.

5. Algar, J., Flynn, J.P. *Proc. R. Ir. Acad.* **1934**, 42B, 1.

6. Oyamada, T. *Bull. Chem. Soc. Jap.*, **1935**, 10, 182-186. https://doi.org/10.1246/bcsj.10.182

7. Nhu, D., Hawkins, B.C., Burns, C.J. *Aust. J. Chem.* **2015**, 68, 1102-1107, https://doi.org/10.1071/CH14620.

8. Geissman, T.A., Fukushima, D.K. *J. Am. Chem. Soc*. **1948**, 70, 1686-1689. https://doi.org/10.1021/ja01185a003

9. Dean, F.M., Podimuang, V. *J. Chem. Soc.* **1965**, 3978-3987. https://doi.org/10.1039/JR9650003978

10. Brady, B.A., O'Sullivan, W.I., Philibin, E.M. *J. Chem. Soc. Chem. Commun*. **1970**, 1435.

11. Donnelly, D.M.X, Lavin, T.P., Melody, D.P., Philbin, E.M. *J. Chem. Soc. (C)* **1971**, 2848.

12. Gao, F., Johnson, K.F., Schlenoff, J.B. *J. Chem. Soc., Perkin Trans*. 2, **1996**, 269-273. https://doi.org/10.1039/P29960000269.

13. Bennett, M., Burke, A.J., O'Sullivan, W.I. *Tetrahedron*, **1996**, 52, 7163-7178. https://doi.org/10.1016/0040-4020(96)00334-1.

14. Gormley, T.R., O'Sullivan, W.I. *Tetrahedron*, **1973**, 12, 369-373. https://doi.org/10.1016/S0040-4020(01)93304-6.

15. Adams, C.J., Main, L. *Tetrahedron*, **1991**, 47, 4979-4990. https://doi.org/10.1016/S0040-4020(01)80961-3.

16. Burke, A.J., O'Sullivan, W.I. *Tetrahedron*, **1997**, 53, 8491-8499.

17. Adams, C.J., Main, L. *Tetrahedron*, **1992**, 48, 9929-9938. https://doi.org/10.1016/S0040-4020(01)92283-5. https://doi.org/10.1016/S0040-4020(97)00506-1.

18. Shen, X., Zhou, Q., Xiong, W., Pu, W., Zhang, W. Zhang, G., Wang, C. *Tetrahedron*, **2017**, 73, 4822-4829. https://doi.org/10.1016/j.tet.2017.06.064.

19. Gao, F., Johnson, K.F., Schlenoff, J.B. *J. Chem. Soc., Perkin Trans. 2,* **1996**, 269-273. https://doi.org/10.1039/P29960000269.

20. Bennett, M., Burke, A.J., O'Sullivan, W.I. *Tetrahedron*, **1998**, 54, 9911-4829. https://doi.org/10.1016/S0040-4020(98)00629-2.

21. Serdiuk, I.E., Roshal, A.D., Blażejowski, *Chem. Het. Comp.* **2015**, 50, 396-403. https://doi.org/10.1007/s10593-014-1487-2.

22. Bunton, C.A., Minkoff, G.J. *J. Chem. Soc.* **1949**, 665-670. https://doi.org/10.1039/JR9490000665

23. Wahlen, J., De Vos, D.E., Jacobs, P.A. *Org. Lett*. **2003**, 5, 1777-1780.

24. Steenackers, B., Neirinckx, A., De Cooman, L., Hermans, I., De Vos, D. *ChemPhysChem.* **2014**, 15, 966-973. https://doi.org/10.1002/cphc.201300981.

25. Maggi, R., Piscopo, C.G., Sartori, G., Storaro, L., Moretti, E. *App. Cat. A: General,* **2012**, 411-412, 146-152. https://doi.org/10.1016/j.apcata.2011.10.032.

26. McDonald, R.N., Steppel, R.N. Dorsey, J.E. *Org. Synth.* (Breslow, R, ed.), John Wiley and Sons, Inc., **1970**, 50, 15-17. https://doi.org/10.1002/0471264180.os050.06.

27. Lowenbien, A. *Ber.* **1924**, 57, 1515-1516. https://doi.org/10.1002/cber.19240570858

28. Saxena, S., Makrandi, J.K., Grover, S.K. *Synthesis,* **1985**, 1, 110-111. 10.1055/s-1985-31130

29. Feurstein, W., st. V. Kostanecki, *Ber.* **1898**, 31, 710-719.

30. Ramakrishnan, V.T., Kagan, J. *J. Org. Chem.* **1970**, 35, 2898-2904. https://doi.org/10.1021/jo00834a010

31. Sousa, S.F., Fernandes, P.A., Ramos, M.J. *J. Phys. Chem. A* **2007**, 111, 42, 10439–10452. https://doi.org/10.1021/jp0734474

32. Becke, A.F. *J. Chem. Phys.* **1993**, 98, 5648–5652. https://doi.org/10.1063/1.464913.

33. Lee, C. Yang, W. Parr, R.G. *Phys. Rev. B*. **1988**, 37, 785-789. https://doi.org/10.1103/PhysRevB.37.785.

34. Grimme, S., Antony, J., Ehrlich, S., Krieg, H. *J. Chem. Phys.* **2010**, 132, 154104. doi.org/10.1063/1.3382344.

35. Grimme, S., Ehrlich, S., Goerigk, L. *J. Comp. Chem*. **2011**, 32, 1456-1465. https://doi.org/10.1002/jcc.21759.

36. Tomasi, J., Mennucci, B., Cammi, R. *Chem. Rev.* **2005**, 105, 8, 2999–3094, https://doi.org/10.1021/cr9904009

37. Riplinger, C., Sandhoefer, B., Hansen, A., Neese, F. *J. Chem. Phys.* **2013**, 139, 134101. https://doi.org/10.1063/1.4821834.

38. Riplinger, C., Neese, F. *J. Chem. Phys.* 2013, 138, 034106, https://doi.org/10.1063/1.4773581.

39. Liakos, D.G., Neese, F. *J. Chem. Theory Comput.* **2015**, 11, 9, 4054–4063. https://doi.org/10.1021/acs.jctc.5b00359